# Atmospheric Rivers in Southern South America

Maximiliano Viale, Instituto Argentino de Nivologia Glaciologia y Ciencias Ambientales, René Garreaud, Universidad de Chile, and F. Martin Ralph, University of California San Diego Scripps Institution of Oceanography Center for Western Weather and Water Extremes

https://doi.org/10.1093/acrefore/9780190228620.013.987

Published online: 20 May 2025

#### Summary

Atmospheric rivers (ARs) are long, narrow bands of strong moisture transport, most often located in the warm sector of extratropical cyclones. The advances in atmospheric science in the early 21st century have demonstrated that ARs are a key component of the climate and the global water cycle by transporting vast amounts of water vapor from tropical/subtropical source regions to extratropical and polar regions. The long and high Andes mountain range, located along the west coast of southern South America, facilitates the conversion of a significant portion of the transported water vapor into precipitation through efficient orographic lifting and orographic precipitation processes. Therefore, atmospheric rivers are a primary regional factor in the climate and the water cycle of southern South America. They are the largest suppliers of water in Patagonia, central Chile, and central western Argentina, as well as the largest generators of extreme precipitation and related hazardous situations (e.g. floods, landslides) over the southern Andes and its surroundings. The understanding of ARs in the southern South America region is still limited compared to other regions in the world; however, some important topics related to atmospheric rivers have been revealed. For example, an AR climatology and its significant contribution to total and extreme precipitation over and around the southern Andes have already been documented, along with some large-scale moisture dynamics in its path over the Pacific Ocean to the continent, as well as the peculiarities of the region related to the differing impacts of ARs given their orientation with respect to the Andes.

Keywords: South America, South Pacific Ocean, extratropical cyclones, water vapor transport, Andes, precipitation, floods

Subjects: Hydrological Cycle, Climate Impact: Extreme Events, Forecasting

## Introduction

ARs are a relatively newly recognized meteorological phenomenon. A formal definition was introduced in 2018 in the glossary of the American Meteorological Society (Ralph et al., 2018): "A long, narrow, and transient corridor of strong horizontal water vapor <a href="https://glossarytest.ametsoc.net/wiki/Water\_vapor">https://glossarytest.ametsoc.net/wiki/Water\_vapor</a> transport that is typically associated with a low-level jet <a href="https://glossarytest.ametsoc.net/wiki/Low-level\_jet">https://glossarytest.ametsoc.net/wiki/Water\_vapor</a> transport that is typically associated with a low-level jet <a href="https://glossarytest.ametsoc.net/wiki/Low-level\_jet">https://glossarytest.ametsoc.net/wiki/Cold\_front</a> of an extratropical cyclone <a href="https://glossarytest.ametsoc.net/wiki/Extratropical\_cyclone">https://glossarytest.ametsoc.net/wiki/Extratropical\_cyclone</a>." Roughly three decades of research in atmospheric moisture transport were necessary to bring small pieces of evidence together and build solid new knowledge about AR formation and its significant implications in the climate system. Since the pioneering studies of Browning and Pardoe (1973) and Zhu and Newell (1998), which provided mesoscale features of AR and suggested global moisture transport from tropical source

Page 1 of 25

regions to deficient extratropical regions is accounted for by transient long and narrow plumes over the ocean basins, there have been a vast number of studies in the in the early 21st century documenting their dynamics and formation, as well as their globally and regionally hydrometeorological impacts. ARs are a key component of the global water cycle, and according to the global AR climatology of Guan and Waliser (2015), the southwestern coast of South America is one of the regions with the largest AR frequency in the world. Conversely, it is one region with the fewest scientific papers devoted to it in the world.

The number of scientific articles focused on ARs has grown rapidly since the first studies at the end of the 1990s (Figure 1). For instance, the number of articles with atmospheric river or AR in the manuscript title ranged from five articles between 1981 and 2000 to 527 between 2014 and 2023 (Figure 1). The topic of ARs has had its own international conference since 2016, with the fourth International AR Conference being held in 2024, and has had special sessions in the large conferences organized by the North American and European Geophysical Unions and Meteorological Societies. Despite the relevance of this phenomenon in South America, the number of articles dealing with their regional aspects is small compared to other regions.

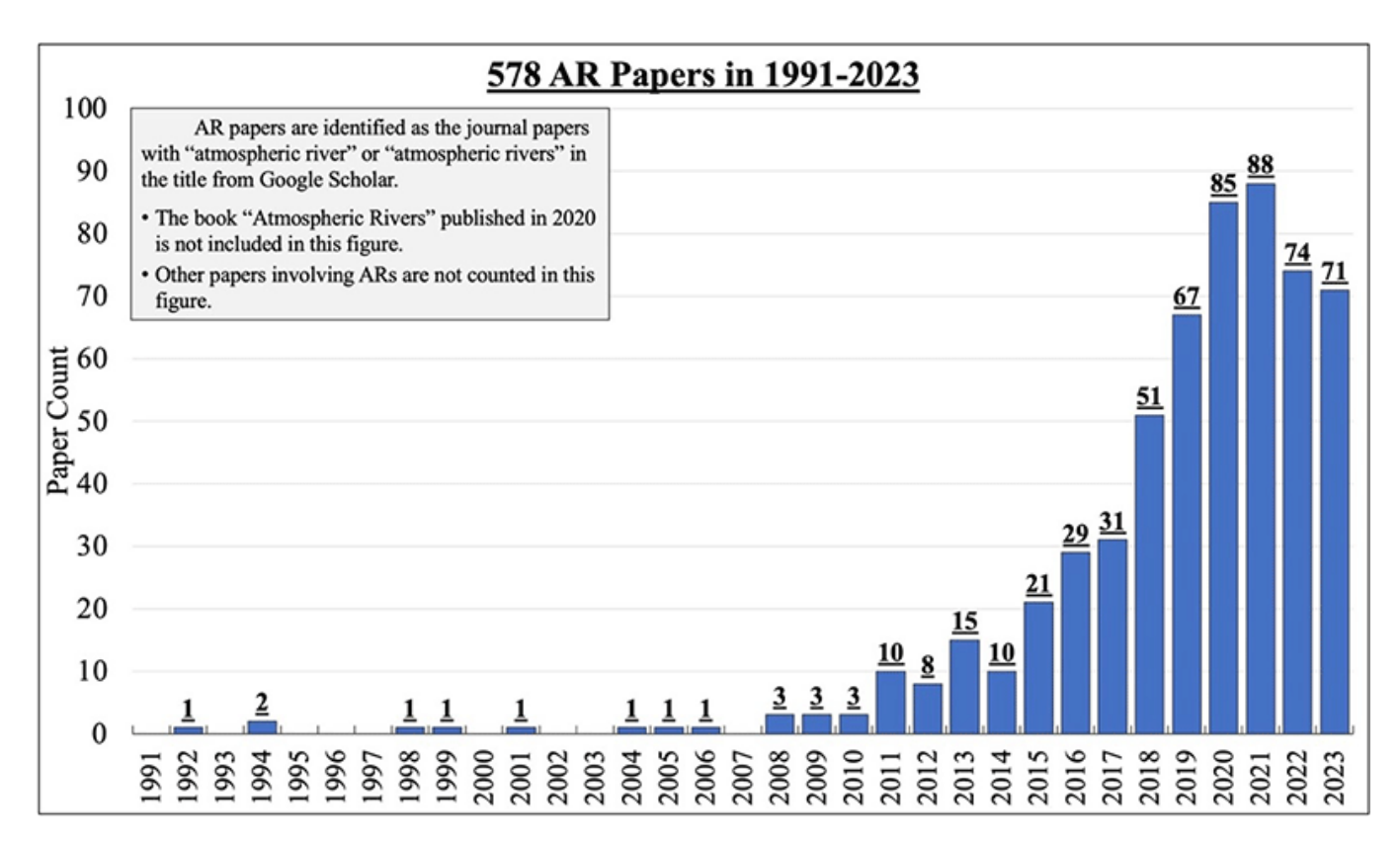


**Figure 1.** Annual count of AR publications in 1991–2023. The AR publications here were identified as the publications with "atmospheric river" or "atmospheric rivers" in the title from peer-reviewed journals according to Google Scholar.

Source: CW3E website.

The main goal of this article is to summarize the current knowledge and advancements related to the AR phenomenon and its hydrometeorological impacts over southern South America. Some new analyses and results on the topics will also be introduced. The key role of ARs in water resources and hydroclimate in the region will be presented in the section "AR as a Key Component of the Water Cycle and Resources in Southern South America." The AR impacts on producing intense and extreme precipitation, which can also often generate flooding, will be discussed in the section "AR Leading to Heavy Precipitation and Hydrometeorological Hazards in Southern South America." Additionally, the characterization of tilted and zonal ARs and their impacts will be presented in the section "Tilted and Zonal ARs in Southern South America." The AR forecast and scale in southern South America and the large–scale dynamics of moisture transport by the ARs over the South Pacific Ocean to the continent are discussed in the sections "AR Category Scale and Forecast in Southern South America" and "Large–Scale Dynamics of Moisture Transport from the Pacific Ocean Through ARs," respectively. Finally, some concluding remarks and future research directions are included in the section "Concluding Remarks and Future Directions in AR–Related Research in Southern South America."

# AR as a Key Component of the Water Cycle and Resources in Southern South America

ARs most often form over the oceans and evolve within the extratropical westerlies. When ARs approach a landmass with coastal mountains, they are forced to ascend over them, causing substantial precipitation in the western margins of the continents. Indeed, ARs are one key component in the hydroclimate of southern South America because of the presence of the Andes along the west coast of the continent. The long meridional extension and the high altitude of the Andes facilitate, through orographic lifting and orographic precipitation processes, the conversion of the water vapor from ARs into liquid and solid particles that grow rapidly to precipitable sizes. Most of the precipitation during the landfall of an AR occurs on the windward (western) side of the Andes, although spillover of hydrometeors also produces precipitation on the leeward (eastern) side of the range, especially in the midlatitudes where the Andes are not as high as at subtropical latitudes (Viale et al., 2019). The sharp precipitation gradient between the more humid western side of the Andes and the drier eastern side is evident in the distinctive landscapes, with dense rainforest on the western Chilean side and desertic steppe on the eastern Argentinean side. Across the southern Andes, Smith and Evans (2007) inferred the highest drying ratio of ~50% for a mountain range through stable isotope analysis from stream water draining on both sides. Despite the precipitation on the Argentinian side being reduced nearly tenfold with respect to the Chilean side, the enhanced orographic precipitation fed by ARs on the Andes and even on the immediate eastern side of the crest provides plenty of water draining down to the lee desert.

One of the first studies highlighting the role of ARs in hydroclimate in South America was Viale and Nuñez (2011). This study focused on the subtropical Andes between 36°S and 30°S, where most of the population in Chile and western Argentina is concentrated. On average, between three and seven intense precipitation events produced by ARs account for most of the water accumulation during the year at these subtropical latitudes, mainly in the form of snow because of the high altitude of the

Andes here (>5,000 m above sea level, ASL) and the relatively low freezing level during winter storms (~2,300 m ASL; Mardones & Garreaud, 2020). These results in the subtropical Andes were later confirmed by snow reanalysis data by Saavedra et al. (2020). The air mass transformation during intense AR precipitation events is very pronounced across the high subtropical Andes, resulting in extremely dry and warm downslope windstorms on the lee side that usually reach the low adjacent lands and cities of Argentina (Viale & Nuñez, 2011). These downslope windstorms are locally known as Zonda winds and often produce severe damage and fatalities (e.g., Norte, 2015). Figure 2 summarizes the principal synoptic conditions during a few heavy precipitation events produced by ARs on the subtropical Andes and that modulate water resources in this region.

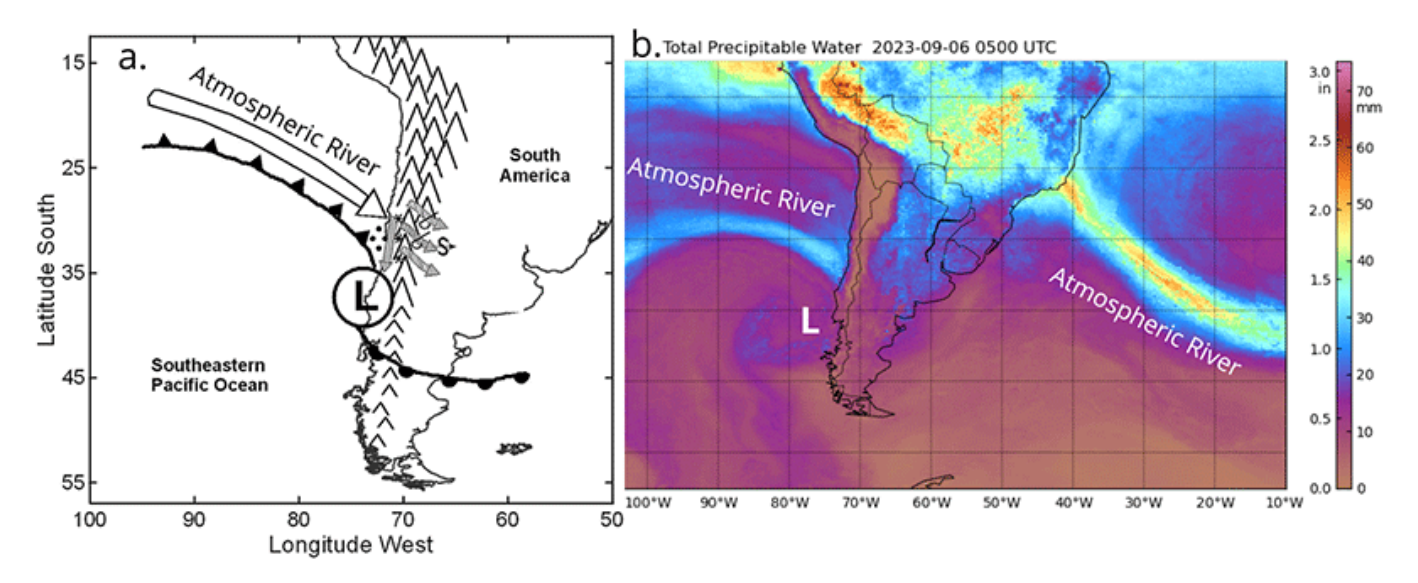


**Figure 2.** (a) Schematic representation of typical synoptic and regional conditions during the heavy orographic precipitation events over the subtropical Andes. The white arrow along the cold front associated with the extratropical cyclone corresponds to an AR toward the Andes, while gray-filled arrows correspond to a barrier jet and downslope flow up and downstream of the Andes, respectively. Typical weather conditions up and downstream of the Andes are indicated by rain, snow, orographic clouds, and downslope "Zonda" windstorm symbols. (b) An example of one AR seen by the MIMIC-TPW2 Satellite product is over the southeastern Pacific Ocean, extending to South America.

Source: Adapted from Viale and Nuñez (2011).

An extension of the AR hydroclimatic impacts along the subtropical and extratropical west coast of South America was brought later by Viale et al. (2018). This study also introduced the first regional climatology of ARs making landfall on the southwest coast of South America. Figure 3a shows that AR frequency peaks between 38°S and 50°S on the Chilean coast, averaging 35–40 days with ARs per year and decreasing rapidly to the south and north of this maximum on the coast, as well as to the east of the Andes in Argentina. Consistent with the pole–to–equator migration of the main westerly wind belt throughout the year, landfalling ARs are more frequent in winter to the north of ~43°S and in summer/autumn to the south of this latitude (Figure 3b and c). The AR climatology was built with an identification algorithm that retains long and narrow plumes with intense water vapor transport (IVT; i.e., greater than the 85th percentile grid–based IVT threshold) from the

Climate Forecast System Reanalysis (CFSR, see Viale et al., 2018). Note that the algorithm also requires that the AR-candidate plumes must overlap or be close to a near-surface frontal zone, defined by a strong horizontal gradient in the 1,000–850 hPa thickness, such that the final identified ARs are linked with midlatitude frontal systems from which the AR phenomenon was initially discovered and for which the formal AR definition was suggested (Ralph et al., 2018).

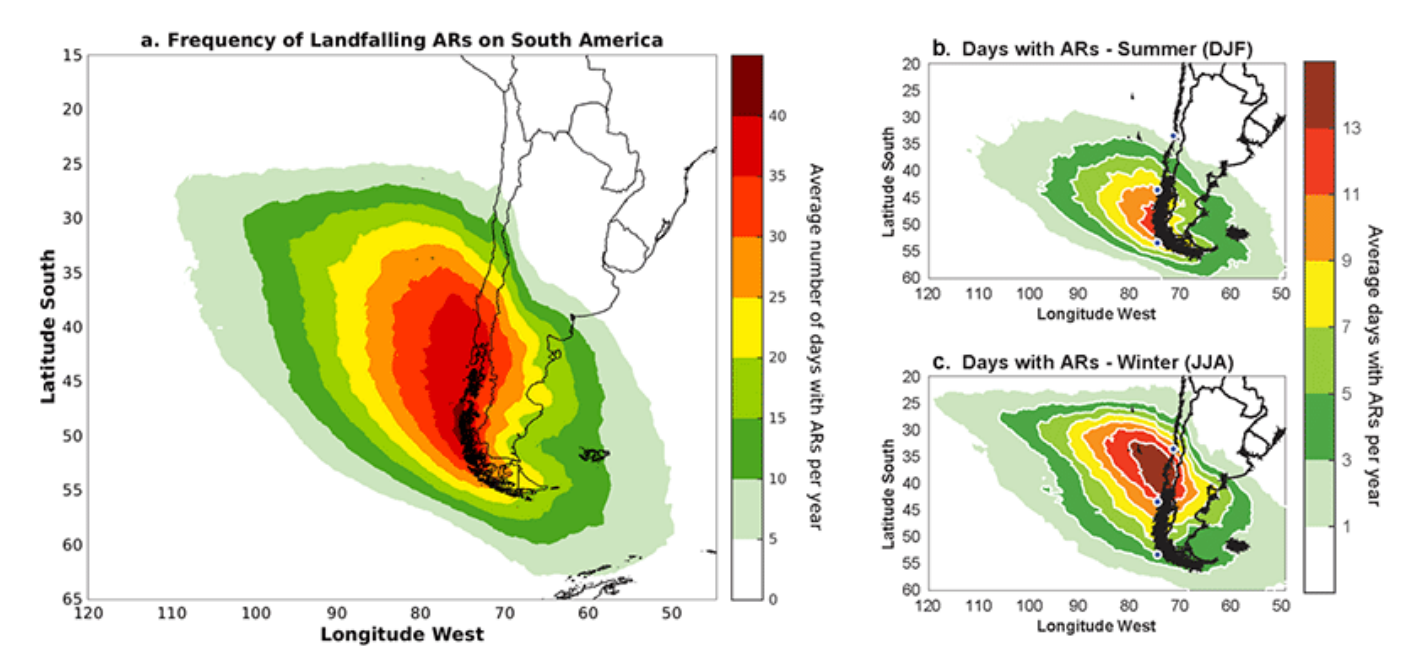


**Figure 3.** (a) Annual, (b) summer (DJF), and (c) winter (JJA) frequencies of landfalling ARs in South America for the 2001–2016 period (presented as average number of days with ARs per year). Blue points are plotted on the coast for reference at 33.5°S (latitude of Santiago), 43.5°S (southern Chiloe Island), and 53.5°S (latitude of Punta Arenas). *Source*: Adapted from Viale et al. (2018).

Combining the AR identification algorithm with surface precipitation gauges in Chile and Argentina, it was quantified the AR impact on precipitation and water resources in southern South America. Figure 4 shows the contribution of AR-produced precipitation to the annual total precipitation, which is greatest on the subtropical west coast, roughly between 32°S and 37°S, and ranging with fraction values of 45% to 65%. This contribution reduces abruptly to the north of 32°S and to the east of the subtropical Andes due to a sharp reduction in AR occurrence. In midlatitudes (37°S to 49°S), the contribution to total annual precipitation is still large from the coast to the immediate east of the Andes crest, with fraction values ranging from 42% to 56% (Figure 4a and c). Farther east on the Patagonia steppe, the AR contribution reduces abruptly despite ARs often penetrating the Andes (Figure 3). South of 50°S, all stations are located east of the austral Andes, so the AR contribution ranges from 40% on the immediate lee sector to less than 15% farther east on the steppe (Figure 4a and d). Compared to studies in the similar mountainous West Coast of North America (Dettinger et al., 2011; Rutz et al., 2014), the AR contribution to total precipitation in South America is very similar, except for subtropical latitudes (30° to 36°), where the Andes are higher than Southern California mountains, and so a stronger orographic effect on AR-related precipitation is expected.

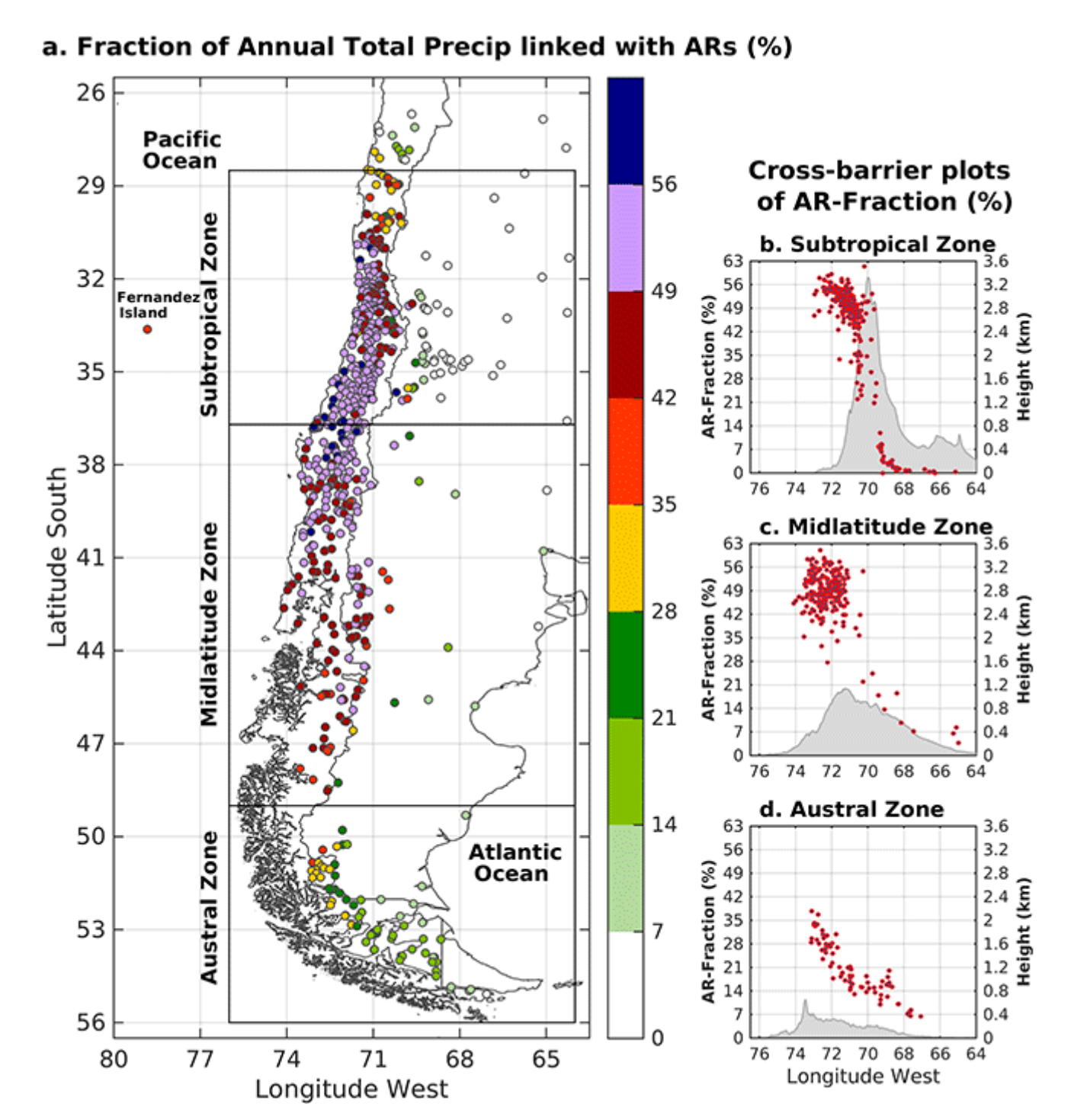


**Figure 4.** (a) Fraction of annual total precipitation associated with AR conditions over the 2001–2016 period. Fractions are multiplied by 100 to express the results in percentage. AR fractions at each station site are calculated using daily rain datasets. Cross-barrier plots of the AR fraction for the (b) subtropical, (c) midlatitude, and (d) austral zones. The limits of each zone are defined in the plan-view plot of (a). The meridionally averaged west-east cross sections of the topography (within the rectangle shown in [a]) are shown in (b–d) as a reference.

Source: Adapted from Viale et al. (2018).

# AR Leading to Heavy Precipitation and Hydrometeorological Hazards in Southern South America

Besides the significant beneficial impact of ARs on water supply in southern South America, strong ARs can produce heavy precipitation events that often lead to flooding, river overflow, and potentially significant damage and fatalities. These negative impacts of ARs can be exacerbated when they impinge on the steep slopes of the Andes, leading also to landslides, avalanches, flash flooding, and other mountainous hydrometeorological hazards. For instance, Corringham et al. (2019) quantified that ARs are the primary drivers of flood damage in the similar mountains of the western United States, and the damage and economic losses increased with the increase of AR duration and intensity (i.e., the AR categories explained below). In southwestern South America, only a few studies provide evidence of AR-related extreme precipitation driving floods and landslides, as summarized here. Additionally, this article includes examples of two powerful ARs that occurred in 2023 but with different thermal conditions, resulting in different significant impacts in the subtropical Andes.

By combining the AR climatology with surface daily and hourly precipitation data, Viale et al. (2018) show that AR storms produce between 1.5 and 3 times more daily precipitation than non-AR storms on the subtropical and midlatitudes zones on the windward side of the Andes (i.e., Chile, Figure 5a). In the austral zone, the ratios of daily precipitation reduce to less than 1.5 because the rain gauges are located east of the Andes crest (i.e., on the leeward side, Figure 5a). On the hourly timescales (Figure 5b−d), precipitation intensity with AR conditions is between two and three times higher than those with non-AR conditions north of 49°S in midlatitudes and subtropical zones. In the austral zone and akin to daily precipitation data, these ratios of hourly precipitation eventually reduce to less than 1 (Figure 5d). When comparing the most intense hourly precipitation (in the fourth quartile) of the AR and non-AR subsets, the ratio of median heavy hourly precipitation indicates both subsets are similar regardless of the AR or non-AR conditions (Figure 5d, yellow dots). Similarly, the most intense daily precipitation (in the fourth quartile) does not correspond 100% to AR precipitation days, roughly 50% to 70% in midlatitudes and subtropical zones (see Figure 11 of Viale et al., 2018), and even a little lower (~50%) for most extreme daily precipitation (above the 95th percentile) as documented by Valenzuela and Garreaud (2019) in similar zones of Chile.

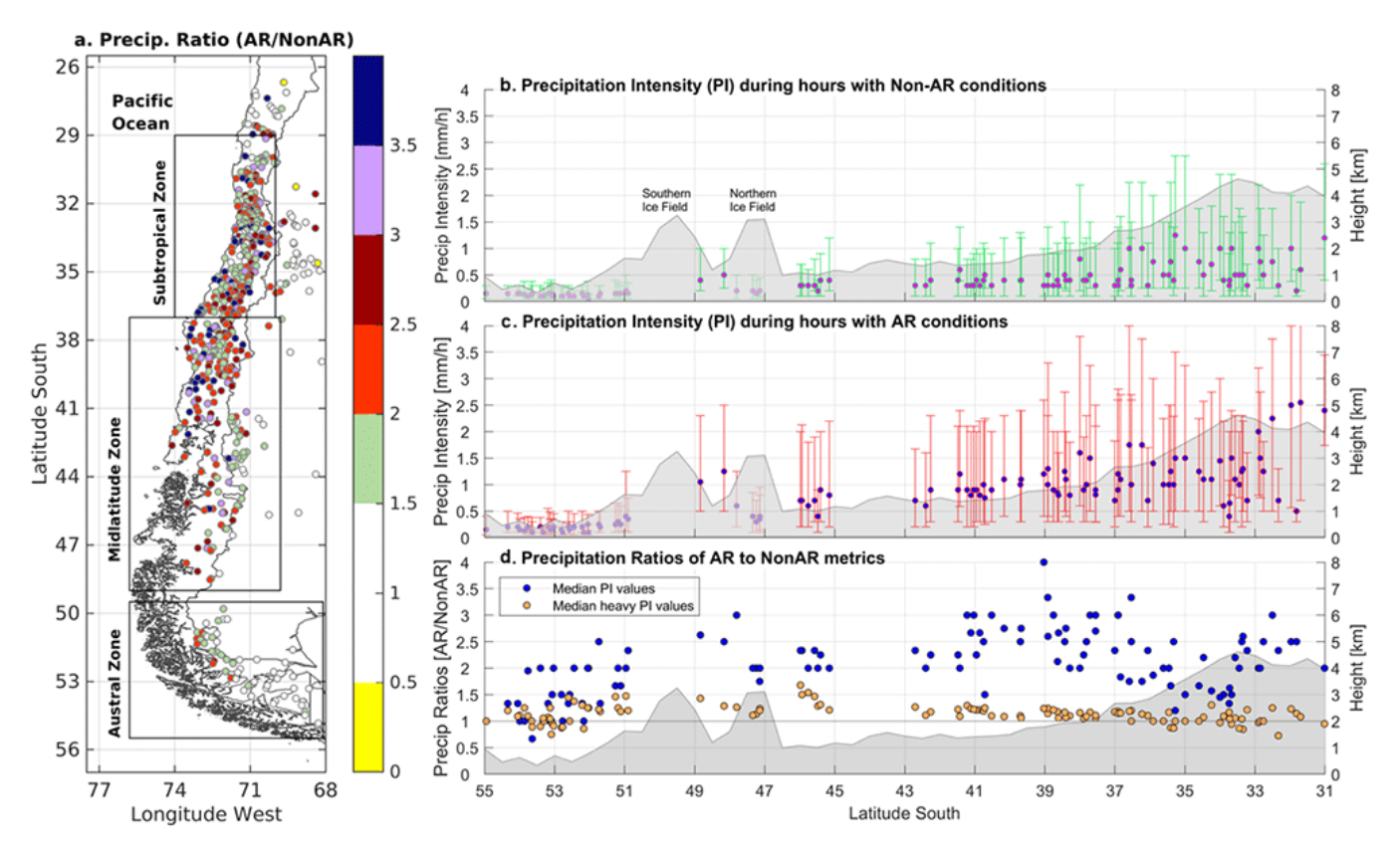


**Figure 5.** (a–Right panel) Ratio of the median of daily precipitation under AR conditions to those under non-AR conditions for the entire years of the 2001–2016 period. Over the 2001–2016 period. (Left panels) Hourly precipitation rates recorded by Chilean surface precipitation on the windward (leeward) side of the Andes during hours with (b) non-AR conditions and (c) AR conditions. Error bars present the median (circle) and 25th and 75th percentile values (whiskers) of each subset. (c) Ratios of median precipitation intensity (blue dots) and mean extreme precipitation intensity (yellow dots) during AR conditions to those during non-AR conditions. Heavy precipitation intensity is defined as hourly precipitation rates within the fourth quartile of each subset. The smoothed topography (km) of the Andes is added in the background for reference. The stations on the lee side of the Andes are plotted behind the topography, which is denoted by the transparency of the area plot. *Source*: Adapted from Viale et al. (2018).

Since ARs can produce heavy precipitation, they can often lead to flooding, debris flow, and landslides, especially on mountainous western continental coastlines such as in North and South America. In North America, since the pioneering study of Ralph et al. (2006), many studies have documented ARs driving floods and landslides (e.g., DeFlorio et al., 2024; Dettinger et al., 2011; Neiman et al., 2011), as well as ARs being the primary source of flooding in the western United States (Barth et al., 2017; Konrad & Dettinger, 2017). Valenzuela et al. (2022) documented how a zonally oriented AR produced an extraordinary precipitation event on the subtropical Andes during the dry summer season, when precipitation is virtually absent. The storm's total precipitation was even larger than in many winter storms. As a result, river flows suddenly increased, and 33 landslides were reported in river basins close to the city of Santiago, affecting over 1,000 people, damaging 400 houses, and blocking many routes, according to local emergency offices.

The other paper showing the high impacts of ARs in South America is Rutllant et al. (2023), which confirmed that 12 extreme precipitation storms producing major floods and/or landslides since 1957 in the Chilean Elqui River basin at 30°S were all driven by ARs. They also showed that despite the relatively low maximum intense water vapor transport (IVT) values in these storms ( $\sim$ 300–400 kg m<sup>-1</sup> s<sup>-1</sup>), compared to the southernmost counterparts, these represent anomalous values higher than 4 to 5 standard deviations from the mean in this very dry subtropical region. According to the AR scale of Ralph et al. (2019), these maximum IVT values correspond to weak or moderate AR categories 1–2 of 5, with beneficial impacts; however, the results of this study in the very dry subtropical west coast of South America suggest that the AR scale could be refined north of  $\sim$ 32°S.

Due to the lack of AR high-impact studies in South America, the analysis of two strong ARs that occurred in 2023 and produced widespread flooding and snowfall is introduced here. Figure 6 shows the weather charts with the sea level pressure and IVT just before the two ARs made landfall between 30°S and 40°S. Both ARs were strong, long-lasting (roughly four days), and primarily zonal oriented, perpendicular to the Andes and so producing substantial upslope flow and precipitation there. Despite all these similarities, they differed in their thermal conditions, which resulted in different hydrometeorological impacts. The AR in late June 2023 was warm, with a mean freezing level at an altitude of 3,300 m above sea level (ASL), producing largely abundant rain over the Andes during four days rather than snow, especially south of 34°S. Rivers draining on both slopes overflowed rapidly, leading to hundreds of route blockages and urban damage. Although there was little snow on this part of the Andes before the warm AR-related rain, a few mountain stations on the Chilean side showed evidence of rain-on-snow melting. Conversely, the AR in August 2023 was cooler and produced abundant snow above 2,500 m in the Andes, leaving many towns and farmers isolated, especially on the lee-side slopes of the Andes.

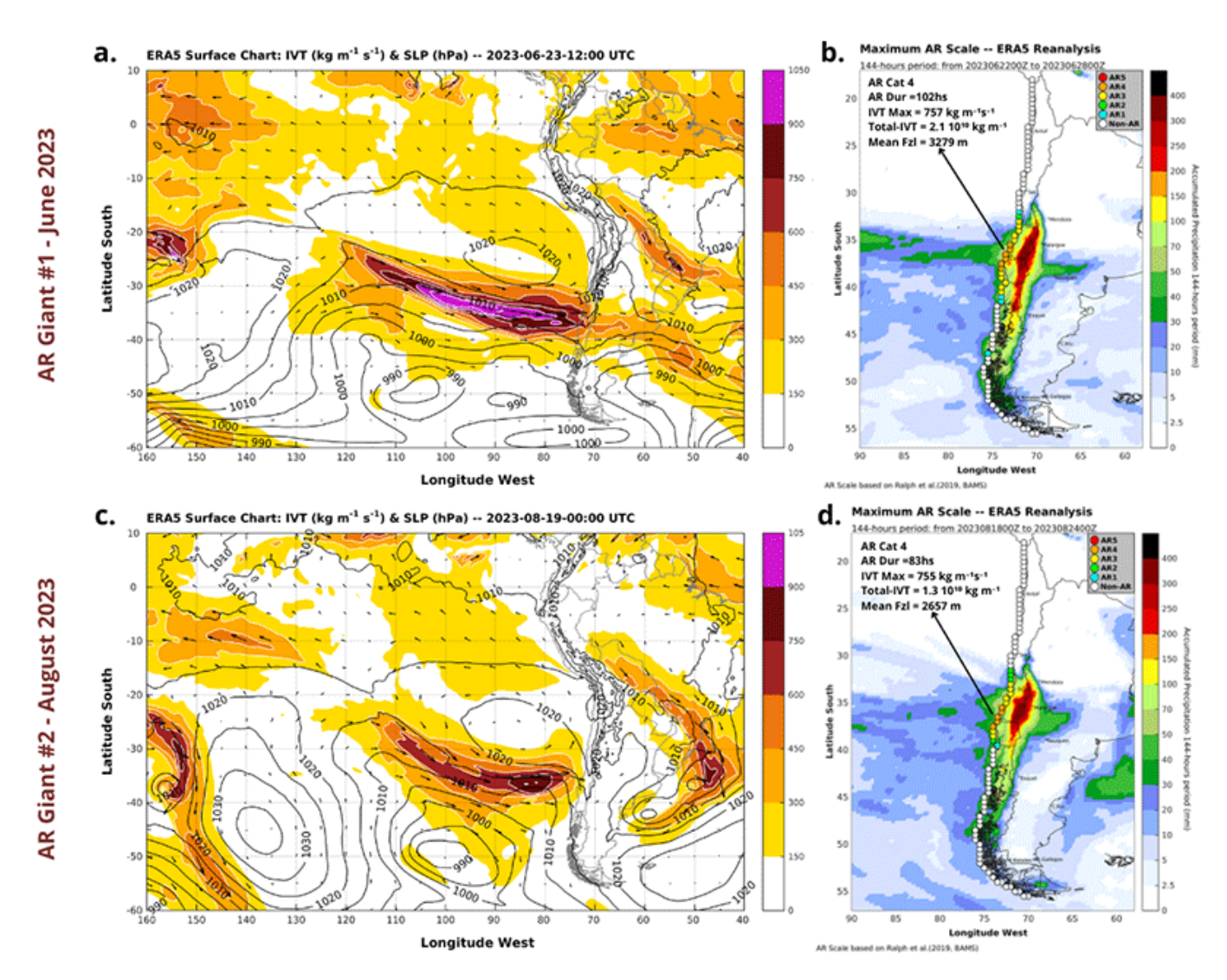


**Figure 6.** (a–c) Surface chart showing the sea level pressure (hPa) and the integrated vapor transport (intense water vapor transport intensity shaded in kg m<sup>-1</sup> s<sup>-1</sup> and direction denoted by the vectors) when two ARs with category 4 made landfall in South America in the same wet season 2023. (b–d) Total-event precipitation reproduced by the ERA5 data. The colored-coded grid points along the coast indicate the category reached by the ARs along the coast, and the text indicates some AR metrics recorded at grid points marked by the black arrows.

During these strong ARs and extreme precipitation events, emergency and disaster states were declared in several regions in Chile and provinces in Argentina. Both events caused massive damage, economic losses, and resulted in missing persons and fatalities in both countries. The extremeness of the precipitation is reflected in several precipitation and streamflow records being broken. The rising daily mean streamflow for the Longavi River, around 35°S in Chile, was the highest since 1940, while for the Neuquén River, around 37°S in Argentina, recorded its the highest since 1902, both during the June AR event (Figure 7a–c). According to the National Weather Services of Chile and Argentina, the stations of Curico and Malargüe, both around 35°S at either foot of the Andes, recorded the highest daily (150 mm) and highest rainy-consecutive-days (183 mm) precipitation events for all time since the 1950s, respectively. Dams in the region of Maule in Chile and the province of Neuquén in Argentina were opened to manage the rapid river overflow and flood risk.

Due to the stratiform nature of the midlatitude frontal precipitation, the resulting floods were not as rapid as the flash floods caused by powerful mesoscale convective precipitation systems normally observed in central Argentina; however, their lengthy, extensive affected areas and strong orographic enhancement of precipitation by the Andes, as denoted by the observations in Figure 7d and e, demonstrate that the amount of water that fell over the Andes was very large.

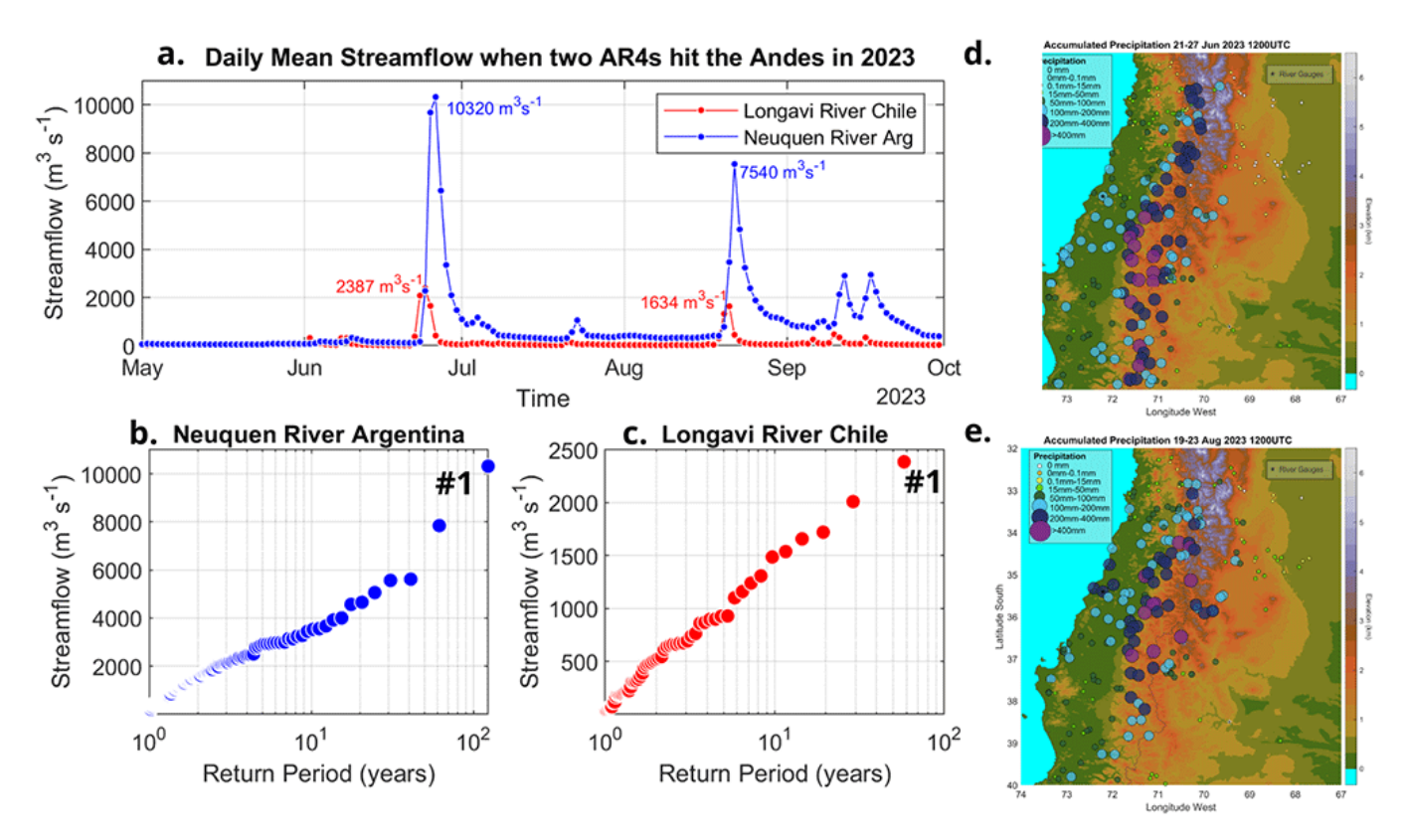


**Figure 7.** (a) Daily mean streamflow time series showing quick extreme rising on both sides of the Andes, for the Longavi River in Chile and the Neuquén River in Argentina, during the 2023 austral winter when two AR categories 4 hit the Andes. (b and c) Return period plot for daily mean streamflow in each river showing that extreme values correspond to the ones registered in 2023. The daily series for Longavi River at the Castillo river-gauge station starts in 1985, while the series for the Neuquén River at the Paso de los Indios river-gauge station starts in 1902. (d and e) Total event precipitation for the two ARs over the subtropical Andes and their surroundings lowlands in Argentina and Chile.

## Tilted and Zonal ARs in Southern South America

Most winter storms in southern South America feature an AR ahead of a cold front, ensuring that low-level air temperatures drop markedly during precipitation as the front progresses equatorward. The arrival of the cold air dome behind the surface front causes a depression of the freezing level from values as large as 3,000 m ASL in the pre-frontal sector to less than 1,500 m ASL in the post-frontal sector. The mean freezing level during precipitation periods generally ranges from 2,000 to 2,300 m ASL, well below the Andes crest level, forming and maintaining the seasonal snowpack that melts in the following spring and summer (Ibañez et al., 2020; Mardones & Garreaud, 2020).

During some winter storms, however, the freezing level remains constant or even rises during the precipitation period, rising above 3,000 m ASL. This results in a larger pluvial area, the part of the watershed that receives rain and produces immediate runoff. Rain at high elevations can trigger landslides and flash floods (e.g., Valenzuela et al., 2022). An extreme case occurred on May 3, 1993, when a moderate precipitation event (25–50 mm of accumulation over the high terrain) was concurrent with a freezing level at about 4,000 m ASL, resulting in numerous landslides in the foothills of the Andes immediately west of Santiago (33°S) that caused over 70 fatalities and thousands of homes to be damaged or lost (Garreaud & Rutllant, 1996). Garreaud (2013) described these so-called winter warm storms and contrasted their synoptic-scale features with the most typical cold storms. These cold storms often feature a tilted AR, while warm storms feature zonal ARs under a strong zonal jet in the middle and upper troposphere.

Valenzuela and Garreaud (2019) focused then on extreme storms in Chile. Two main synoptic-scale patterns were found for stations south of 35°S. The most frequent cases feature a well-defined cold front, strong northwest flow in the mid-troposphere, and often a tilted AR. In contrast, the less-frequent cases feature a more zonal circulation and AR, along with warmer temperatures during the precipitation period, quite consistent with Garreaud (2013). For instance, the extraordinary precipitation event during the summer dry season highlighted before was driven by a zonal AR (Valenzuela et al., 2022).

At that time, it became clear that zonal atmospheric rivers (ZARs) were distinct and more hazardous than the more common NW-SE-oriented atmosphere rivers (referred to as tilted cases or TARs). That prompted a study targeting ZARs and TARs reaching south-central Chile that used case studies and composite analysis of 31 ZAR and 67 TAR cases, respectively, between 2000 and 2020 (Garreaud et al., 2024). During the most common TARs (Figure 8a-c), the low- and mid-level circulations show a low-pressure system and trough moving rapidly eastward, respectively, and NW winds over south-central Chile. Downstream of the trough axis, there is a broad region of mid-tropospheric ascent and a surface low, thus conforming to a typical baroclinic wave reaching the west coast of extratropical South America. In the ZAR cases (Figure 8b-d), there is tropospheric-deep zonal flow across much of the Pacific and WSW winds off central Chile. The zonal tongue of high moisture originates at low latitudes far from the Chilean coast, near the entrance region of a zonal jet that swiftly transports water vapor eastward. The ZAR runs parallel to a quasi-stationary front, and precipitation is concentrated between the coast and the crest of the Andes upstream, where orographic uplift plays a dominant role. These contrasting synoptic-scale patterns of the ZAR composite are also illustrated in Figure 8.

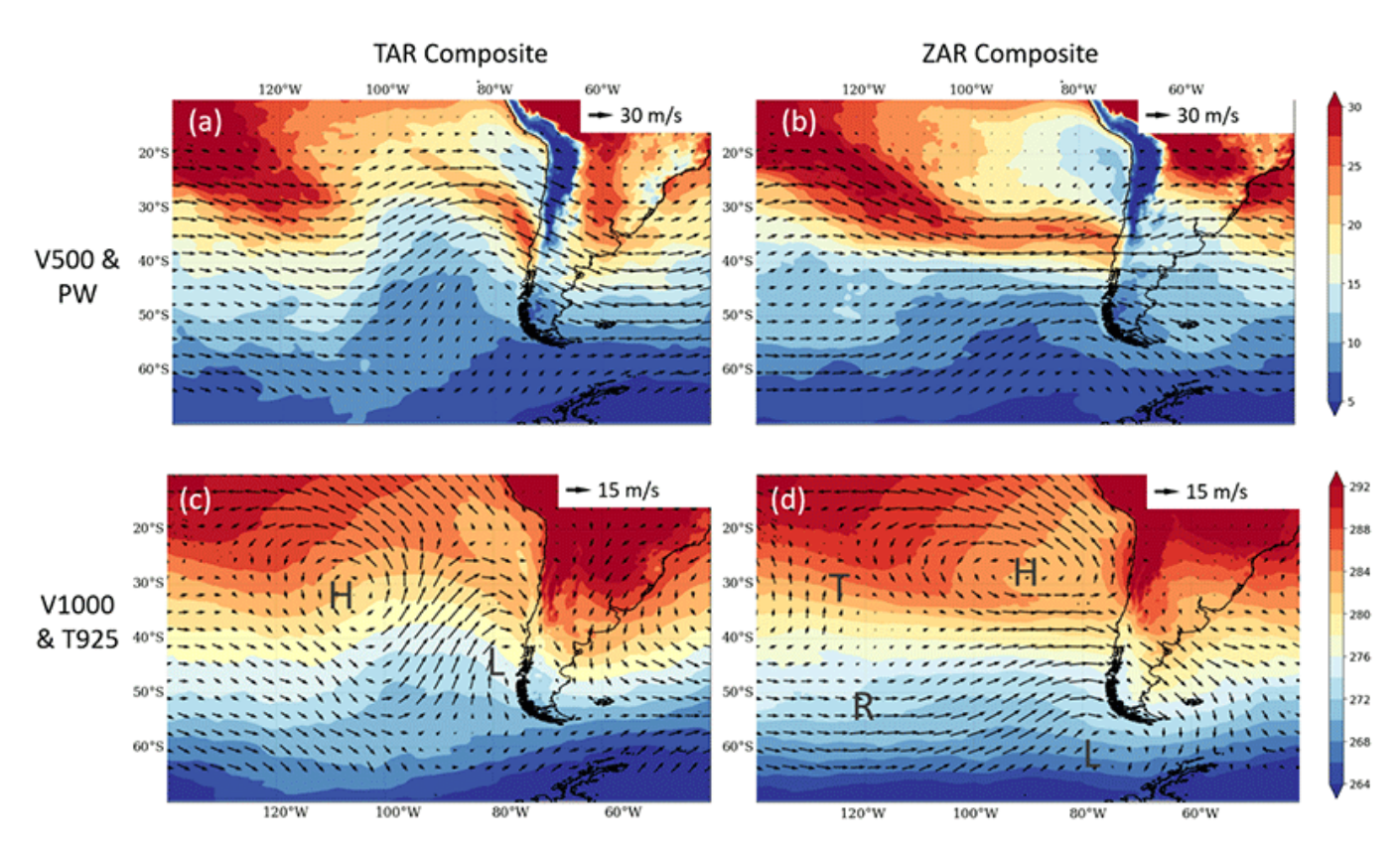


**Figure 8.** Large-scale circulation for the (a–c) TAR and (b–d) ZAR groups. The upper panels show each group's composite 500-hPa wind vectors and precipitable water (colors, mm). The lower panels show each group's composite 1,000-hPa wind vectors and 92- hPa air temperature (colors, mm). Some surface features are identified for guidance: L = low, H = subtropical high, R = Ridge, and T = Trough. All variables from ERA5.

Source: Figure from Garreaud et al. (2024).

The large-scale environment of a ZAR sets the stage for high hydrometeorological hazards (Garreaud et al., 2024). During a ZAR landfall, the lower-middle tropospheric winds are nearly perpendicular to the Andes, maximizing the moisture flux against the sloping terrain. This explains the augmented orographic precipitation during these events compared to the TAR cases, in which the moisture flux impinges at an oblique angle against the Andes (Garreaud et al., 2024). On average, a ZAR exhibits an orographic precipitation enhancement approximately 50% greater than the average of the tilted ARs, thus causing more precipitation over the western slope of the Andes for a comparable level of intense water vapor transport magnitude (Figure 9). Studies of ARs in other regions have also recognized the relevance of the AR direction in rainfall accumulation in mountainous coastal areas (e.g., Griffith et al., 2020; Hecht & Cordeira, 2017).

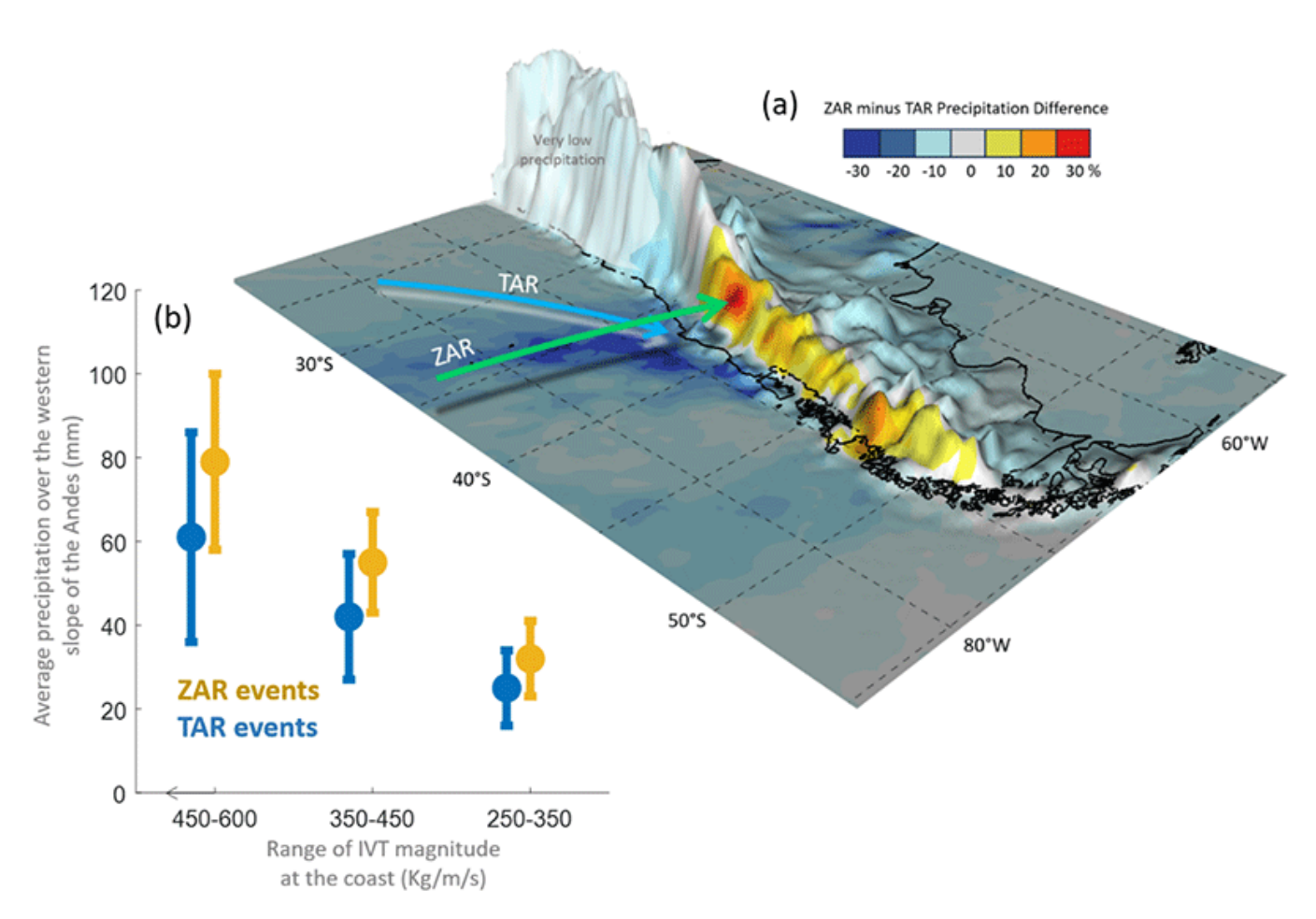


**Figure 9.** (a) The difference between the mean precipitation in 31 ZAR cases and the mean precipitation in 67 TAR cases. The cases were selected by Garreaud et al. (2024) based on the IVT magnitude and upper wind direction. The difference was divided by the average of all cases and expressed in percentages. The green and cyan arrows represent the central axis along the ZAR and TAR, respectively. (b) Mean ± 1 standard deviation of the precipitation over the elevated terrain of the Biobio region (37°S–38°S, 71.6°W–71.1°W, mean elevation 1,690 m ASL) for ZAR and TAR events, stratified in three categories of IVT magnitude at the coast. Note that IVT increases to the left.

 $\it Source$ : Figure from Garreaud et al. (2024).

Furthermore, because of its location ahead of the stationary front, the band where a ZAR makes landfall tends to persist in a narrow range of latitudes for two to three days, causing persistent precipitation, as occurred in the extraordinary precipitation event of 2023 shown previously. Furthermore, most precipitation occurs during a period with warm temperatures in the lower and middle troposphere. In some cases, the arrival of the ZAR causes an increase in air temperature and the freezing level, as illustrated in Figure 10 with data from the Atmospheric River Observatory in Concepción, Chile, a coastal city at 36°S, for the case that occurred in mid–July 2022. The combination of longevity, warm conditions, and enhanced orographic precipitation during landfalling ZARs may explain the occurrence of major disasters along south–central Chile, such as the fatal landslides in Santiago in May 1993 (Garreaud & Rutllant, 1996) and Villa Santa Lucia in December 2017, as well as the widespread flooding in July 2006 (Garreaud, 2013) and June 2023.

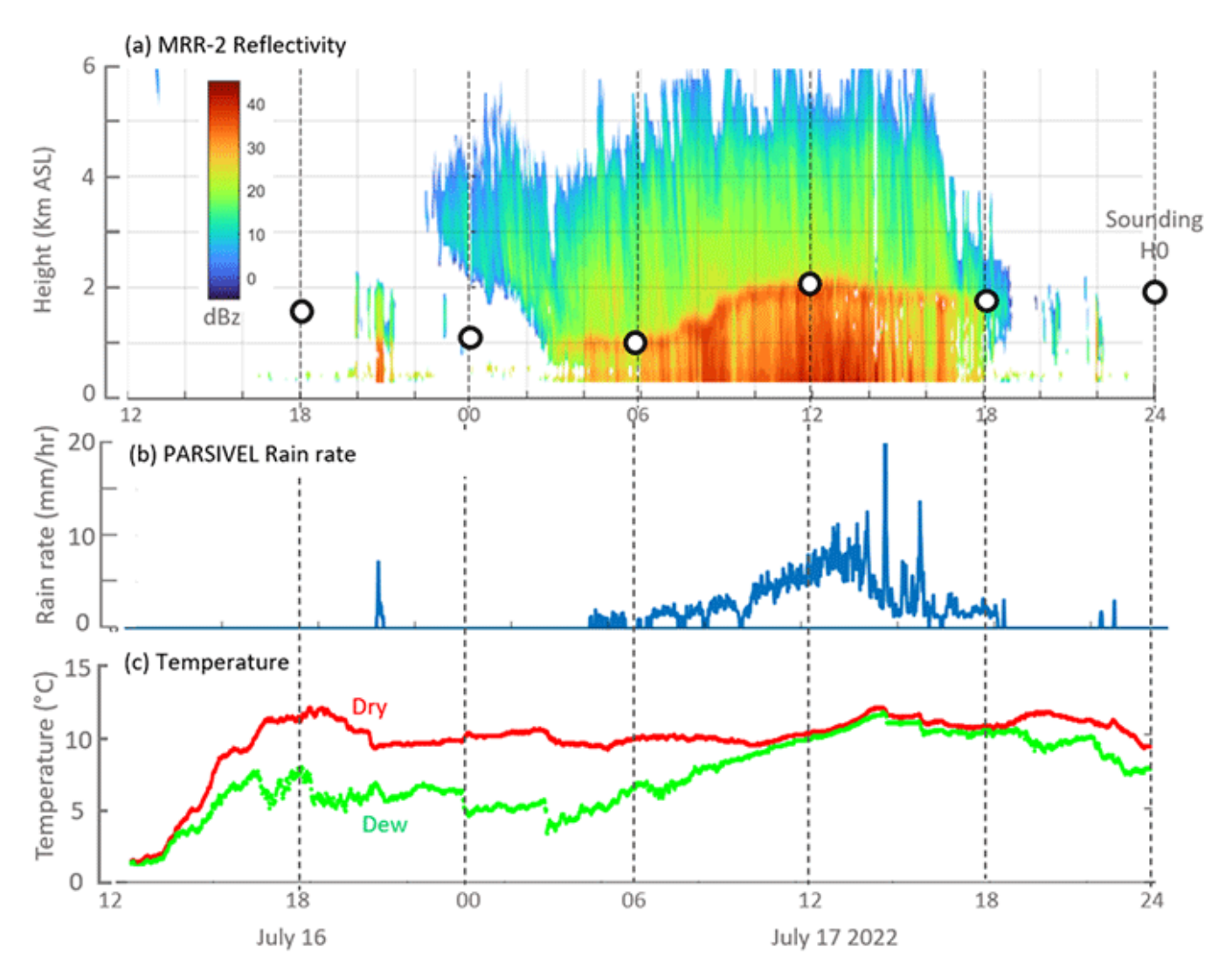


**Figure 10.** The passage of a ZAR ahead of a stationary front during July 16–17, 2022, as seen from the Atmospheric River Observatory in Concepción (36.8°S, 73°W, 25 m ASL). (a) Radar reflectivity profiles acquired by a Micro-Rain-Radar (MRR-2). The white dots indicate the sounding derived 0°C isotherm height. (b) Minute rain intensity measured by a PARSIVEL-2 Disdrometer; (c) Minute air temperature (red) and dew point (green). Note the rise in the freezing level during the precipitation period.

Source: Figure from Garreaud et al. (2024).

Figure 11 shows the polar plot of the 500-hPa winds over Concepción (37°S, 71°W) for days with precipitation at this coastal location in southern Chile. The direction of the mid-level wind over the coast is a proxy for the orientation of the along-AR axis and hence allows for discrimination between zonal (i.e.,  $u >> |v| \sim 0$ ) and tilted (i.e.,  $|v| \geq u$ ) ARs (Garreaud et al., 2024). According to Figure 11, most ARs landfalling in southern Chile are tilted (see also Valenzuela & Garreaud, 2019), impinging at an oblique angle against the Andes. Only a minor fraction of ARs have a zonal orientation, thus producing large orographic enhancement on the Andes. Similarly, most of the ARs landfalling in western North America are tilted (oriented from SW to NE), as illustrated by the polar plot of the 500-hPa winds over San Francisco (38°N, 128°W). Nonetheless, the main axis of the

Sierra Nevada and the coastal mountains runs NW-to-SE, maximizing the orographic lifting of moisture flux over that range during the more frequent TARs, resulting in higher orographic precipitation (e.g., see Figure 4 of Hecht & Cordeira, 2017).

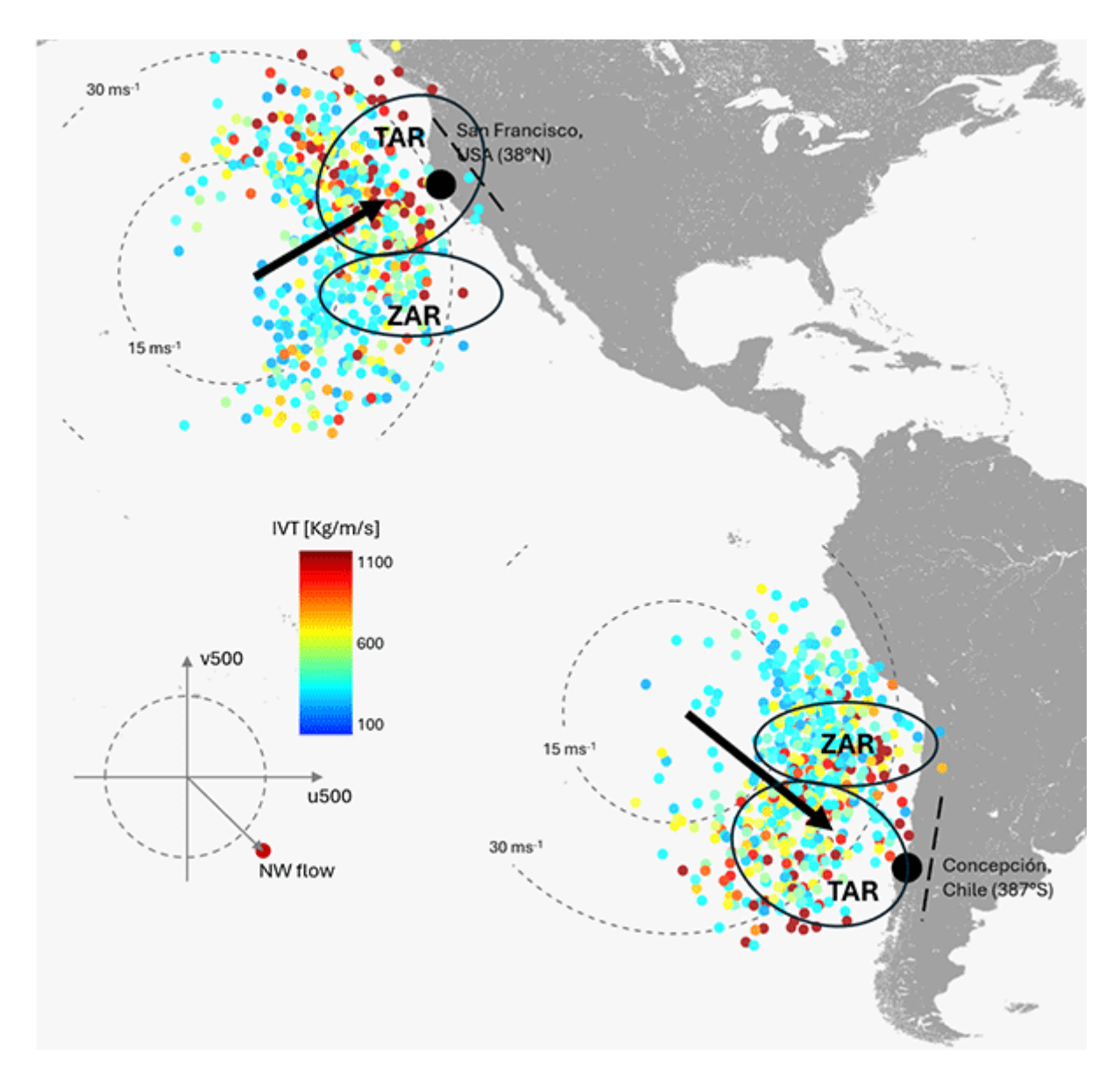


**Figure 11.** Polar plot of the 500-hPa winds over Concepción, Chile (37°S, 71°W) and San Francisco, United States (38°S, 123°W). Both locations are indicated by the black circle, but the polar plots are displaced to the left on the map for clarity. The black dashed line indicates the main axis of the Andes or Sierra Nevada at the corresponding latitude. Each dot represents the wind at 12 Coordinated Universal Time (UTC) for each day of the corresponding winter between 2000 and 2020. The dots are colored according to the IVT magnitude on that day. The key on the lower-left side gives an example of a day with winds blowing from the NW and high IVT. The 500-hPa wind direction is a proxy of the orientation of the AR main axis from where the events are classified as ZAR (zonal cases) or TAR (tilted cases).

Source: Data from ERA5.

## **AR Category Scale and Forecast in Southern South America**

Since ARs are predominantly responsible for extreme precipitation and floods in the western midlatitude continents and big islands (e.g., Ralph & Dettinger, 2012, in North America; Ramos et al., 2015, in the Iberian Peninsula; Kingston et al., 2016, in New Zealand; and Lavers et al., 2011, in the United Kingdom), the forecast for ARs coming from the vast ocean basins becomes an important precursor. Indeed, it has been demonstrated that the numerical weather prediction models predict better the IVT of ARs over the North Pacific and Atlantic Oceans than the associated extreme precipitation in the western United States and United Kingdom (Lavers et al., 2014, 2016). This was an expected result because moisture transport over the ocean is mainly tied to synoptic–scale processes, while extreme precipitation is connected to localized or mesoscale processes, such as the atmosphere–terrain interaction or frontal convergence. Consequently, the higher predictability of IVT, especially within ARs and compared to heavy precipitation, makes the forecasts based on water vapor transport a highly valuable tool for providing earlier situational awareness of extreme precipitation associated with ARs.

In southern South America, a brief model validation of an extreme precipitation forecast caused by an AR anticipated a potential intense precipitation event seven days before it, but with nonnegligible changes in its intensity and location in the Andes during lead times closer to the event (see Figures 10 and 11 of Valenzuela et al., 2022). The precipitation forecast limitations in the Globlal Forecast System (GFS) global model in this case, which occurred in January 2021, raise doubts for forecasters about the extremity of the forecasted precipitation event, which might be mitigated by also looking at the AR forecast. The limitations in the orographic precipitation forecasts by the global models motivated the development of a specific website, with focused forecast products on ARs coming from the Pacific Ocean toward southern South America. The website was developed at the Instituto Argentino de Nivología, Glaciología y Ciencias Ambientales\_<a href="https://ianiqla.net/">https://ianiqla.net/</a> rios\_atmosfericos/>. The website was also motivated by all previous AR science, including the higher predictability of IVT than precipitation, as well as by the broad use of the AR-hydrometeorological website provided by the Center for Western Weather and Water Extreme at the Scripps Institution of Oceanography at the University of California, San Diego in North America. AR forecasts are a valuable tool for predicting extreme precipitation and flood awareness, and they play an important role in, among other things, water management, risk assessment, and decision-making.

One newly available AR forecast product is the AR category scale from Ralph et al. (2019). The AR scale uses the IVT maximum value during the period when IVT continuously exceeds 250 kg m<sup>-1</sup> s<sup>-1</sup>, which, in turn, establishes the AR duration at a given geographic location. The combination of AR intensity and duration determines the AR rankings from 1 to 5, with 1 being the shorter and weaker ARs, with mostly beneficial impacts of water supply, and 5 being the longer and stronger ARs, with mostly hazardous impacts such as floods and landslides. Like the five-category hurricane scale, the AR scale is simple to apply and easily interpreted by all kinds of users. The AR scale is operationally implemented on the website for AR forecasts in southern South America, along with other products and visualizations, as exemplified in Figure 5 for two extreme precipitation events driven by AR category 4 in 2023.

The frequency of the AR categories along the southwest coastline of South America over the 53-year (1970–2022) period, according to the ERA5 reanalysis data (Hersbach et al., 2023), is shown in Figure 12. The coastal grid points where the AR category frequencies were examined are plotted in Figure 6b–d. All AR category occurrences maximize south of 40°S and drop abruptly north of 40°S (Figure 12a). This result obtained from a Eulerian approach at grid points (i.e., the time series of conditions at a fixed geographic location) closely aligns with the frequency of ARs identified as objects or areas with strong IVT (see Figure 3a from Viale et al., 2018). To the north of 30°S (Figure 12b), AR conditions are rarely reached in any AR categories, including the lowest category, AR 1, which occurs less than once per year (or once every several years). Recall that this subtropical sector of the west coast is very dry (i.e., the Atacama Desert region), strongly influenced by subsidence circulation from the semipermanent Southeastern Pacific Subtropical Anticyclone. This is why AR conditions defined by the fixed threshold of 250 IVT units (i.e., kg m<sup>-1</sup> s<sup>-1</sup>) represent large anomalous moisture transport here, as highlighted by Rutllant et al. (2023).

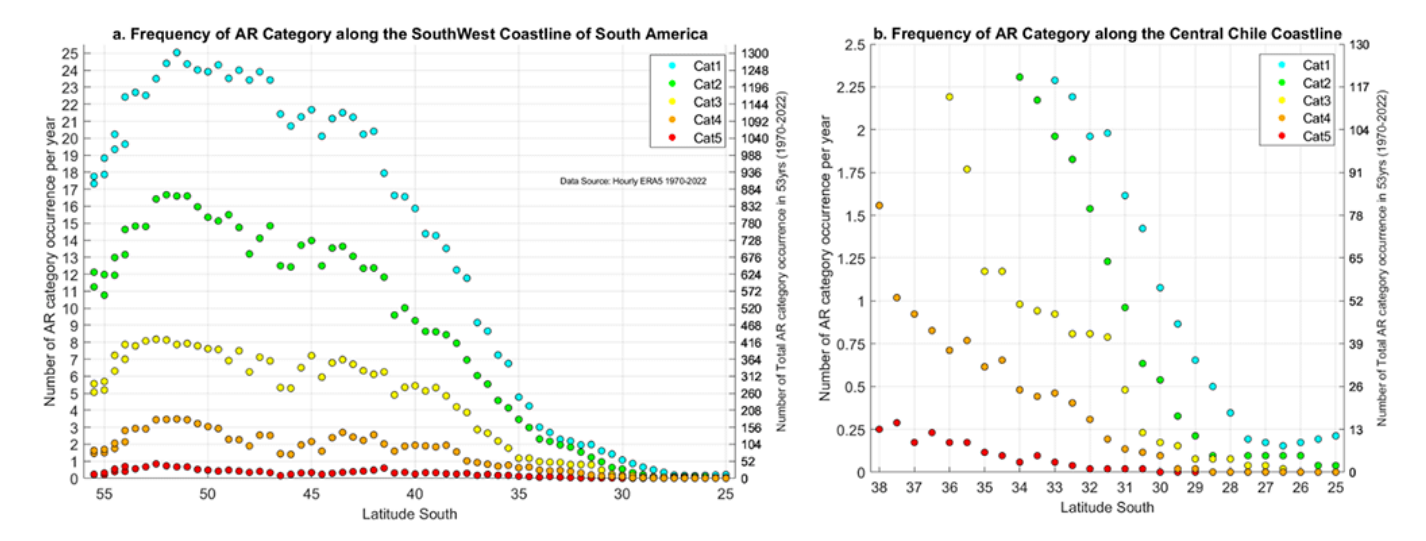


**Figure 12.** (a) Frequency of AR categories along the southwestern coast of South America over the period 1970–2022 using ERA5 reanalysis data. For the grid point locations along the coastline, see Figure 5b–d. (b) Same as (a) but zoomed into the central Chile coastline sector where most of the population of Chile and western Argentina are concentrated.

# Large-Scale Dynamics of Moisture Transport from the Pacific Ocean Through ARs

Recent results of the large-scale dynamic processes explaining the water vapor transport from the South Pacific Ocean to the continent through ARs are reviewed here. Akin to other AR-related topics, the number of papers on AR large-scale processes is small compared to other regions with larger atmospheric science communities. To our knowledge, only four papers cover the interannual variability of large-scale moisture transport to the dynamics of moisture transport in different subsectors of the southeastern Pacific Ocean that reach the South American continent.

They demonstrated that during the warm ENSO phase, El Niño, a corridor of enhanced westerly transport of water vapor over the South Pacific Ocean, is established, setting the stage for a higher frequency of ARs reaching the central sector of Chile, including long-lasting zonal cases. Therefore, there is more precipitation in central Chile and the subtropical Andes compared to the winter climatology and the cold ENSO phase, La Niña. This corridor is part of the previously documented large-scale circulation pattern over the South Pacific in response to the anomalous heating of the central equatorial Pacific Ocean and triggered Rossby wave train (e.g., Rutllant & Fuenzalida, 1991); however, the moist large-scale dynamics in this so-called Pacific-South American pattern had not been analyzed prior to the recent study by Campos and Rondanelli (2023).

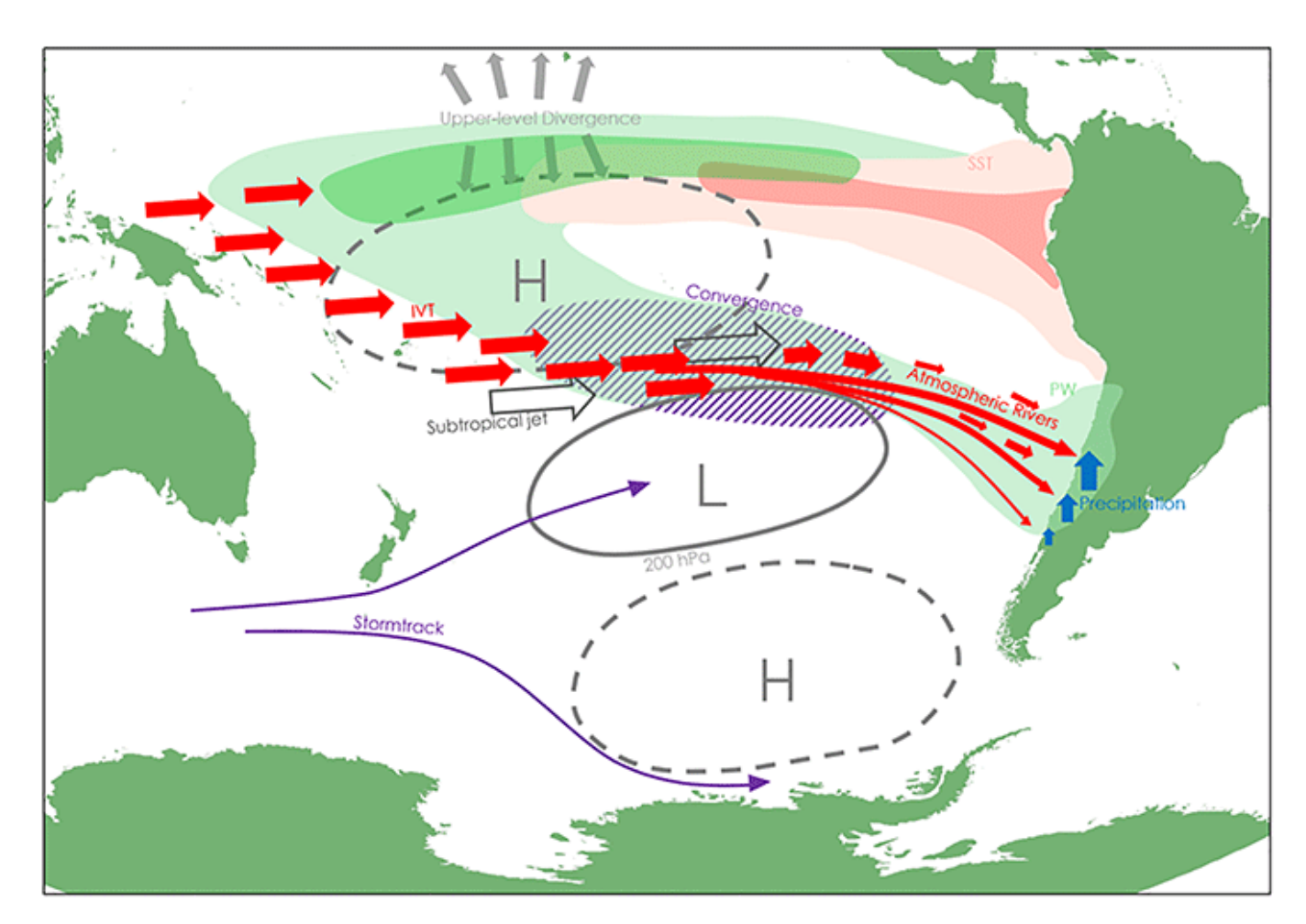


**Figure 13.** Schematic of the Pacific-South American pattern with the large-scale corridor of enhanced westerly moisture transport which favors higher frequency of ARs across central Chile and subtropical Andes.

Source: Figure from Campos and Rondanelli (2023).

The novel study of Mudiar et al. (2024) provides a better understanding of the moisture dynamics in ARs through a moisture budget of 50 ARs over the South Pacific Ocean that reached South America and produced significant precipitation upon landfall in the Andes. Figure 14 from this study highlights its main findings. Convergence of tropical/subtropical moist air masses forms and

maintains the long plume with significant water vapor content over the open ocean. This convergence of moist air is in balance with precipitation, but near the coast, the advection of moisture and precipitation becomes more important in the moisture budget. The convergence of moist air forming the AR is normally driven by the anticyclonic circulation from the semipermanent subtropical high pressure and cyclonic circulation from extratropical cyclones.

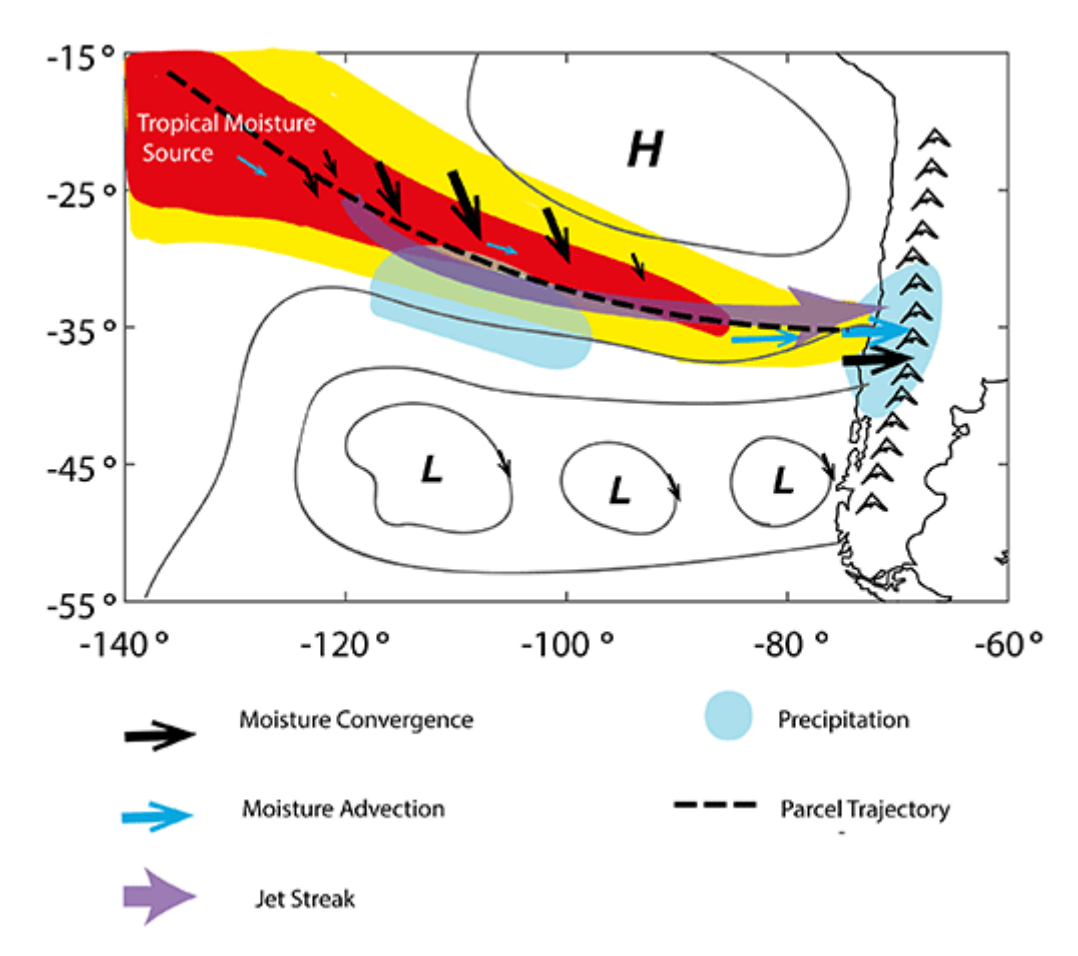


**Figure 14.** Schematic diagram showing the result of Lagrangian moisture budgets of air column within zonal landfalling AR in the southern Andes. The shaded areas indicate integrated water vapor along the AR channel. The symbols H and L indicate the location of a subtropical anticyclone and a midlatitude lows.

Source: Figure from Mudiar et al. (2024).

Another relevant result of the moisture transport dynamics has been shown by Böhm et al. (2021). This study reveals that moisture transport from the Pacific Ocean during rare precipitation events in the Atacama Desert does not occur near the surface as it typically occurs ahead of midlatitude frontal systems; instead, it occurs in mid-level troughs that are decoupled from the maritime boundary layer. The case study of Vicencio Veloso (2022) also suggests this mid-level moisture dynamic, which, in turn, is coherent with previous studies documenting that frontal systems usually do not reach this sector of subtropical west coast of South America (Seluchi et al., 2006). The study of Böhm et al. (2021) further showed that a great proportion of moisture in mid-level AR-like plumes that produce precipitation on the western side of the subtropical Andes, in the Atacama

Desert, comes from the other side of the Andes in the Amazon basin. This is likely to be possible in the tropics with warmer temperatures, where the Clausius-Clapeyron relationship allows much more moisture to overpass the tropical Andes.

# Concluding Remarks and Future Directions in AR-Related Research in Southern South America

In the early 21st century, the great progress in atmospheric science has demonstrated that ARs are a key component of the climate and the global water cycle. Their key global role is transporting huge amounts of water vapor in the atmosphere from tropical/subtropical source regions to extratropical and polar sink regions. By transporting water vapor, ARs transport potential latent heat and potential liquid or solid water far away, which take effect if they condensate and precipitate to the ground. Mountain ranges, especially large and high ones such as the Andes, facilitate these water vapor conversion processes, so ARs are a primary regional factor in climate and the water cycle in southern South America. ARs are the largest suppliers of water in Patagonia and central Chile and central western Argentina, and they are the largest generators of extreme precipitation and related hazardous situations (e.g., floods, landslides) over the southern Andes and its surroundings. ARs fuel orographic precipitation in the Andes, where efficient orographic precipitation processes are activated. In other words, the Andes Mountain range facilitates the landing of these great rivers in the sky onto the ground.

This article has reviewed the knowledge of AR science in the southern South America region and introduced some new results. Since the atmospheric science community is small in southern South America, the number of scientific articles on ARs and their related topics is smaller than in other regions. Nonetheless, this review addresses articles that have covered major topics on ARs in relation to the characteristics of the region. Results that documented the climatology of ARs and their significant contribution (50% to 60%) to total precipitation and water supply, as well as their linkage with stronger precipitation events at daily and hourly scales, were summarized first. Then, some examples were presented of powerful, giant ARs that produced extreme precipitation in the southern Andes, record-breaking river streamflow, and widespread flooding with massive damage and even fatalities. Finally, progress in understanding the differing impacts of ARs based on their orientation with respect to the Andes was also summarized, along with advances in the large-scale moisture dynamics associated with ARs forming and moving over the South Pacific basin.

Despite these advances, there remains a lack of knowledge regarding AR-related science in southern South America. For instance, investigations of ARs driving hydrometeorological hazardous impact in different river basins of the Andes are much needed in the region. The Andes span a large range of latitudes and altitudes, featuring a diverse array of river basins in terms of orientation and steepness, bedrocks and soil composition, vegetation, snow, and glacier coverages that surely modulate different responses to the AR and extreme precipitations. The interaction between AR-related precipitation and the cryosphere on the Andes is also a big topic without much attention yet. An article published in 2025 pointed out the key role that AR-related precipitation

events may have on annual glacier balances (Bravo et al., 2024). In conclusion, atmospheric research around ARs and their impacts is still in its early stages in South America, whereas in other parts of the world, it has flourished for years.

#### References

Barth, N. A., Villarini, G., Nayak, M. A., & White, K. (2017). Mixed populations, and annual flood frequency estimates in the western United States: The role of atmospheric rivers. *Water Resources Research*, *53*, 257–269.

Böhm, C., Reyers, M., Knarr, L., & Crewell, S. (2021). The role of moisture conveyor belts for precipitation in the Atacama Desert <a href="https://doi.org/10.1029/2021gl094372">https://doi.org/10.1029/2021gl094372</a>. Geophysical Research Letters, 48(24).

Bravo, C., Cisternas, S., Viale, M., Paredes, P., Bozkurt, D., & García-Lee, N. (2024). Unseasonal atmospheric river drives anomalous glacier accumulation in the ablation season of the subtropical Andes <a href="https://doi.org/10.5194/egusphere-2024-1958,%202024">https://doi.org/10.5194/egusphere-2024-1958,%202024</a>. EGUsphere [preprint].

Browning, K. A., & Pardoe, C. W. (1973). Structure of low-level jet streams ahead of mid-latitude cold fronts <a href="https://doi.org/10.1002/qj.49709942204">https://doi.org/10.1002/qj.49709942204</a>. Quarterly Journal of the Royal Meteorological Society, 99(422), 619–638.

Campos, D., & Rondanelli, R. (2023). ENSO-related precipitation variability in central Chile: The role of large-scale moisture transport <a href="https://doi.org/10.1029/2023JD038671">https://doi.org/10.1029/2023JD038671</a>. Journal of Geophysical Research: Atmospheres, 128(17), e2023JD038671.

Corringham, T. W., Ralph, F. M., Gershunov, A., Cayan, D. R., & Talbot, C. A. (2019). Atmospheric rivers drive flood damages in the western United States <a href="https://doi.org/10.1126/sciadv.aax4631">https://doi.org/10.1126/sciadv.aax4631</a>. Science Advances, 5(12), eaax4631.

DeFlorio, M. J., et al. (2024). From California's extreme drought to major flooding: Evaluating and synthesizing experimental seasonal and subseasonal forecasts of landfalling atmospheric rivers and extreme precipitation during winter 2022/23 <a href="https://doi.org/10.1175/BAMS-D-22-0208.1">https://doi.org/10.1175/BAMS-D-22-0208.1</a>>. Bulletin of the American Meteorological Society, 105, E84–E104.

Dettinger, M. D., Ralph, F. M., Das, T., Neiman, P. J., & Cayan, D. (2011). Atmospheric rivers, floods and the water resources of California <a href="https://doi.org/10.3390/w3020445">https://doi.org/10.3390/w3020445</a>. Water, 3, 445–478.

Garreaud, R. (2013). Warm winter storms in central Chile. Journal of Hydrometeorology, 14, 1515–1534.

Garreaud, R., & Rutllant, J. (1996). Análisis meteorológico de los aluviones de Antofagasta y Santiago de Chile en el periodo 1991–1993. *Atmosfera*, 9, 251–271.

Garreaud, R. D., Jacques-Coper, M., Marín, J. C., & Narváez, D. A. (2024). Atmospheric rivers in south-central Chile: Zonal and tilted events <a href="https://doi.org/10.3390/atmos15040406">https://doi.org/10.3390/atmos15040406</a>. Atmosphere, 15(4), 406.

Griffith, H. V., Wade, A. J., Lavers, D. A., & Watts, G. (2020). Atmospheric river orientation determines flood occurrence <a href="https://doi.org/10.1002/hvp.13905">https://doi.org/10.1002/hvp.13905</a>. Hydrological Processes, 34(23), 4547–4555.

Guan, B., & Waliser, D. E. (2015). Detection of atmospheric rivers: Evaluation and application of an algorithm for global studies <a href="https://doi.org/10.1002/2015jd024257">https://doi.org/10.1002/2015jd024257</a>. Journal of Geophysical Research: Atmospheres, 120(24), 12514–12535.

Hecht, C. W., & Cordeira, J. M. (2017). Characterizing the influence of atmospheric river orientation and intensity on precipitation distributions over North Coastal California <a href="https://doi.org/10.1002/2017GL074179">https://doi.org/10.1002/2017GL074179</a>. Geophysical Research Letters, 44(17), 9048–9058.

Hersbach, H., Bell, B., Berrisford, P., Biavati, G., Horányi, A., Muñoz Sabater, J., Nicolas, J., Peubey, C., Radu, R., Rozum, I., Schepers, D., Simmons, A., Soci, C., Dee, D., & Thépaut, J.-N. (2023). *ERA5 hourly data on single levels from 1940 to present* <a href="https://doi.org/10.24381/cds.adbb2d47">https://doi.org/10.24381/cds.adbb2d47</a>. Copernicus Climate Change Service (C3S) Climate Data Store (CDS).

Ibañez, M., Gironás, J., Oberli, C., Chadwick, C., & Garreaud, R. D. (2020). Daily and seasonal variation of the surface temperature lapse rate and 0°C isotherm height in the western subtropical Andes <a href="https://doi.org/10.1002/joc.6743">https://doi.org/10.1002/joc.6743</a>. International Journal of Climatology, 41(S1).

Kingston, D. G., Lavers, D. A., & Hannah, D. M. (2016). Floods in the southern Alps of New Zealand: The importance of atmospheric rivers <a href="https://doi.org/10.1002/hyp.10982">https://doi.org/10.1002/hyp.10982</a>. Hydrological Processes, 30, 5063–5070.

Konrad, C. P., & Dettinger, M. (2017). Flood runoff in relation to water vapor transport by atmospheric rivers over the western US, 1949–2015 <a href="https://doi.org/10.1002/2017GL075399">https://doi.org/10.1002/2017GL075399</a>. Geophysical Research Letters, 44, 11456–11462.

Lavers, D. A., Allan, R. P., Wood, E. F., Villarini, G., Brayshaw, D. J., & Wade, A. J. (2011). Winter floods in Britain are connected to atmospheric rivers <a href="https://doi.org/10.1029/2011GL049783">https://doi.org/10.1029/2011GL049783</a>. Geophysical Research Letters, 38, L23803.

Lavers, D. A., Pappenberger, F., & Zsoter, E. (2014). Extending medium-range predictability of extreme hydrological events in Europe <a href="https://doi.org/10.1038/ncomms6382">https://doi.org/10.1038/ncomms6382</a>. Nature Communications, 5, 5382.

Lavers, D. A., Waliser, D. E., Ralph, F. M., & Dettinger, M. (2016). Predictability of horizontal water vapor transport relative to precipitation: Enhancing situational awareness for forecasting western U.S. extreme precipitation and flooding ≤https://doi.org/10.1002/2016GL067765>. Geophysical Research Letters, 43, 2275–2282.

Mardones, P., & Garreaud, R. D. (2020). Future changes in the free tropospheric freezing level and rain–snow limit: The case of central Chile <a href="https://doi.org/10.3390/atmos11111259">https://doi.org/10.3390/atmos11111259</a>. Atmosphere, 11(11), 1259.

Mudiar, D., Rondanelli, R., Valenzuela, R. A., & Garreaud, R. D. (2024). Unraveling the dynamics of moisture transport during atmospheric rivers producing rainfall in the southern Andes *≤https://doi.org/10.1029/2024GL108664>*. *Geophysical Research Letters*, *51*(13), e2024GL108664.

Neiman, P., Schick, L. J., Ralph, F. M., Hughes, M., & Wick, G. A. (2011). Flooding in western Washington: The connection to atmospheric rivers <a href="https://doi.org/10.1175/2011JHM1358.1">https://doi.org/10.1175/2011JHM1358.1</a>. Journal of Hydrometeorology, 12, 1337–1358.

Norte, F. (2015). Understanding and forecasting Zonda wind (Andean foehn) in Argentina: A review <a href="https://doi.org/10.4236/acs.2015.53012">https://doi.org/10.4236/acs.2015.53012</a>. Atmospheric and Climate Sciences, 5, 163–193.

Ralph, F. M., & Dettinger, M. (2012). Historical and national perspectives on extreme west coast precipitation associated with atmospheric rivers during December 2010. <a href="http://journals.ametsoc.org/doi/abs/10.1175/BAMS-D-11-00188.1">http://journals.ametsoc.org/doi/abs/10.1175/BAMS-D-11-00188.1</a>> Bulletin of the American Meteorological Society, 93, 783–790.

Ralph, F. M., Dettinger, M. D., Cairns, M. M., Galarneau, T. J., & Eylander, J. (2018). Defining atmospheric river: How the glossary of meteorology helped resolve a debate <a href="https://doi.org/10.1175/BAMS-D-17-0157.1">https://doi.org/10.1175/BAMS-D-17-0157.1</a>. Bulletin of the American Meteorological Society, 99, 837–839.

Ralph, F. M., Neiman, P. J., Wick, G. A., Gutman, S. I., Dettinger, M., Cayan, D., & White, A. (2006). Flooding on California's Russian River: Role of atmospheric rivers <a href="https://doi.org/10.1029/2006GL026689">https://doi.org/10.1029/2006GL026689</a>. Geophysical Research Letters, 33, L13801.

Ralph, F. M., Rutz, J. J., Cordeira, J. M., Dettinger, M., Anderson, M., Reynolds, D., & Smallcomb, C. (2019). A scale to characterize the strength and impacts of atmospheric rivers <a href="https://doi.org/10.1175/BAMS-D-18-0023.1">https://doi.org/10.1175/BAMS-D-18-0023.1</a>. Bulletin of the American Meteorological Society, 100(2), 269–289.

Ramos, A. M., Trigo, R. M., Liberato, M. L., & Tomé, R. (2015). Daily precipitation extreme events in the Iberian Peninsula and its association with atmospheric rivers. <a href="http://journals.ametsoc.org/doi/abs/10.1175/JHM-D-14-0103.1">http://journals.ametsoc.org/doi/abs/10.1175/JHM-D-14-0103.1</a> Journal of Hydrometeorology, 16, 579–597.

Rutllant, J., & Fuenzalida, H. (1991). Synoptic aspects of the central Chile rainfall variability associated with the southern oscillation <a href="https://doi.org/10.1002/joc.3370110105"><a href="https://doi.org/10.1002/joc.3370110105"></a>. International Journal of Climatology, 11, 63–76.

Rutllant, J. A., Matus, F., Rudloff, V., & Rondanelli, R. (2023). The role of atmospheric rivers in rainfall-induced landslides: A study from the Elqui valley <a href="https://doi.org/10.1016/j.jaridenv.2023.105016">https://doi.org/10.1016/j.jaridenv.2023.105016</a>. Journal of Arid Environments, 216, 105016.

Rutz, J. J., Steenburgh, W. J., & Ralph, F. M. (2014). Climatological characteristics of atmospheric rivers and their inland penetration over the western United States. *Monthly Weather Review*, *142*, 905–921.

Saavedra, F., Cortés, G., Viale, M., Margulis, S., & McPhee, J. (2020). Atmospheric rivers contribution to the snow accumulation over the Southern Andes (26.5° S–37.5° S) <a href="https://doi.org/10.3389/feart.2020.00261">https://doi.org/10.3389/feart.2020.00261</a>. Frontiers in Earth Science, 8.

Seluchi, M. E., Garreaud, R., Norte, F. A., & Saulo, A. (2006). Influence of the subtropical Andes on baroclinic disturbances: A cold front case study. <a href="http://journals.ametsoc.org/doi/abs/10.1175/MWR3247.1">http://journals.ametsoc.org/doi/abs/10.1175/MWR3247.1</a> Monthly Weather Review, 134, 3317–3335.

Smith, R. B., & Evans, J. P. (2007). Orographic precipitation and water vapor fractionation over the Southern Andes <a href="https://doi.org/10.1175/jhm555.1">https://doi.org/10.1175/jhm555.1</a>. Journal of Hydrometeorology, 8(1), 3−19.

Valenzuela, R., & Garreaud, R. (2019). Extreme daily rainfall in central-southern Chile and its relationship with low-level horizontal water vapor fluxes <a href="https://doi.org/10.1175/JHM-D-19-0036.1">https://doi.org/10.1175/JHM-D-19-0036.1</a>. Journal of Hydrometeorology, 20, 1829–1850.

Valenzuela, R., Garreaud, R., Vergara, I., Campos, D., Viale, M., & Rondanelli, R. (2022). An extraordinary dry season precipitation event in the subtropical Andes: Drivers, impacts, and predictability <a href="https://doi.org/10.1016/j.wace.">https://doi.org/10.1016/j.wace.</a> 2022.100472>. Weather and Climate Extremes, 37, 100472.

Viale, M., Bianchi, E., Cara, L., Ruiz, L. E., Villalba, R., Pitte, P., Masiokas, M., Rivera, J., & Zalazar, L. (2019). Contrasting climates at both sides of the Andes in Argentina and Chile <a href="https://doi.org/10.3389/fenvs.2019.00069">https://doi.org/10.3389/fenvs.2019.00069</a>>. Frontiers in Environmental Science, 7, 69.

Viale, M., & Nuñez, M. N. (2011). Climatology of winter orographic precipitation over the subtropical Central Andes and associated synoptic and regional characteristics. *Journal of Hydrometeorology*, *12*, 481–507.

### **Atmospheric Rivers in Southern South America**

Viale, M., Valenzuela, R., Garreaud, R., & Ralph, F. M. (2018). Impacts of atmospheric rivers on precipitation over the southern South America <a href="https://doi.org/10.1175/JHM-D-18-0006.1">https://doi.org/10.1175/JHM-D-18-0006.1</a>. Journal of Hydrometeorology, 19, 1671–1687.

Vicencio Veloso, J. (2022). Analysis of an extreme precipitation event in the Atacama Desert in January 2020 and its relationship to humidity advection along the Southeast Pacific. *Atmosfera*, *35*(3), 421–448.

Zhu, Y., & Newell, R. E. (1998). A proposed algorithm for moisture fluxes from atmospheric rivers. *Monthly Weather Review*, *126*, 725–735.